Structure of Fibrinogen in Electrolyte Solutions Derived from Dynamic Light Scattering (DLS) and Viscosity Measurements

ARTICLE *in* LANGMUIR · MARCH 2009

Impact Factor: 4.46 · DOI: 10.1021/la803662a · Source: PubMed

3 AUTHORS:

Monika Wasilewska
Instytut Katalizy i Fizykochemii Powierzch…
17 PUBLICATIONS **348** CITATIONS
SEE PROFILE

Zbigniew Adamczyk
Akademickie Centrum Komputerowe CYFR…
177 PUBLICATIONS **3,707** CITATIONS
SEE PROFILE

Barbara Jachimska
Polish Academy of Sciences
38 PUBLICATIONS **623** CITATIONS
SEE PROFILE

Article

Structure of Fibrinogen in Electrolyte Solutions Derived from Dynamic Light Scattering (DLS) and Viscosity Measurements

Monika Wasilewska, Zbigniew Adamczyk, and Barbara Jachimska

Langmuir, **2009**, 25 (6), 3698-3704• DOI: 10.1021/la803662a • Publication Date (Web): 19 February 2009

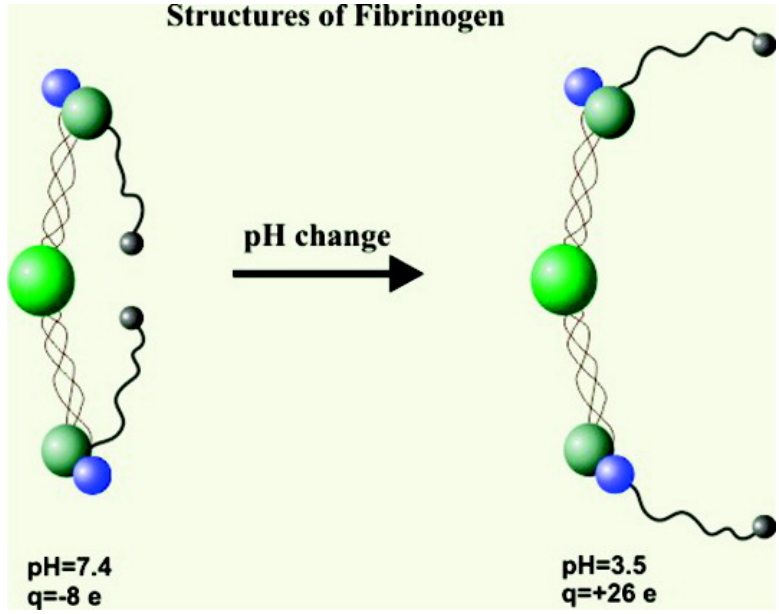

More About This Article

Additional resources and features associated with this article are available within the HTML version:

- Supporting Information
- Access to high resolution figures
- Links to articles and content related to this article
- Copyright permission to reproduce figures and/or text from this article

View the Full Text HTML

Structure of Fibrinogen in Electrolyte Solutions Derived from Dynamic Light Scattering (DLS) and Viscosity Measurements

Monika Wasilewska,* Zbigniew Adamczyk, and Barbara Jachimska

Institute of Catalysis and Surface Chemistry, Polish Academy of Science, Niezapominajek 8, 30-239 Cracow, Poland

Received November 4, 2008. Revised Manuscript Received January 17, 2009

Bulk physicochemical properties of bovine plasma fibrinogen (Fb) in electrolyte solutions were characterized. These comprised determination of the diffusion coefficient (hydrodynamic radius), electrophoretic mobility, and isoelectric point (iep). The hydrodynamic radius of Fb for the ionic strength of 0.15 M was 12.7 nm for pH 7.4 (physiological conditions) and 12 nm for pH 9.5. Using these values, the number of uncompensated (electrokinetic) charges on the protein N_c was calculated from the electrophoretic mobility data. It was found that for physiological condition (pH 7.4, $I = 0.15$), $N_c = -7.6$. For pH 9.5 and $I = 10^{-2}$, $N_c = -26$. On the other hand, N_c became zero independent of the ionic strength at pH 5.8, which was identified as the iep. Consequently, for pH <5.8, N_c attained positive values, approaching 26 for lower ionic strength and pH 3.5. It was also found from the hydrodynamic diameter measurements that for a pH range close to the iep, that is, 4−7, the stability of Fb suspension was very low. These physicochemical characteristics were supplemented by dynamic viscosity measurements, carried out as a function of Fb bulk volume concentration, for various pH values. Using these experimental data the contour length of 80 nm was predicted for Fb molecules in electrolyte solutions. On the other hand, the effective length of the molecule was 53−55 nm for physiological conditions, which suggested a collapsed state of the terminal chains. However, for the range of pH outside the iep, its effective length increased to 65−68 nm. This was interpreted in terms of a significant unfolding of the terminal chains of Fb caused by electrostatic repulsion. The effective charge, contour length, and effective length data derived in this work seem to be the first of this type reported in the literature.

Introduction

The desire to predict, manipulate, and control biopolymer adsorption and especially protein immobilization processes has been the main driving force for researchers in the past two decades. Protein adsorption is crucial in the fields of biotechnology, food processing, biosensors, and disease diagnostic.[1−6] Well-ordered protein layer deposition requires a thorough knowledge of their behavior in bulk solution, especially the shape of the molecules, their conformations state, charge, and mobility properties. All of this information can be obtained using noninvasive hydrodynamic methods, for example, dynamic light scattering (DLS), dynamic viscosity,[7] circular dichroism (CD),[8] and fluorescence depolarization measurements. Another step in the examination of protein adsorption state is imaging of protein molecules on the surface. Atomic force microscopy with intermittent contact mode (semicontact) is a very useful and versatile device that can be applied to imaging of various biological molecules such as proteins.[9,10]

Numerous studies have been concerned with fibrinogen (Fb)[12−17] because of its fundamental role in blood clotting. Fibrinogen is a large plasma glycoprotein with a molecular mass of 340 kDa, consisting of two sets of three nonidentical polypeptide chains (α, β, and γ).[18] It is the third most prevalent protein in plasma, with a concentration of 2.6−3 mg/mL.[19] It is also one of the most relevant proteins that is adsorbed on biomaterial surfaces. Its native structure has been described by Hall and Slayter,[20] who used electron microscopy to propose a trinodular structure (three hydrophobic domains connected by α-helical coiled coil domains) with an overall molecular length of 47.5 nm. Fibrinogen is a key protein in the regulation of both thrombosis and haemostasis.[4,21−24]

Because of the significance of Fb deposition, many studies have been carried out, mostly with the aim of determining the structure of the molecule and its dimensions in the adsorbed state, which was mostly done using a variety of AFM meth-

* Corresponding author (e-mail ncwasile@cyf-kr.edu.pl).

(1) Martin, B. D.; Gaber, B. P.; Patterson, C. H.; Turner, D. C. *Langmuir* **1998**, *14*, 3971.
(2) Rezwan, K.; Meier, L. P.; Rezwan, M.; Voros, J.; Textor, M.; Gauckler, L. J. *Langmuir* **2004**, *20*, 10055.
(3) Desroches, M.; Chaudhary, N.; Omanovic, S. *Biomacromolecules* **2007**, *8*, 2836.
(4) Brash, J. L.; Horbett, T. A. *Proteins at Interfaces: Physicochemical and Biochemical Studies*; ACS Symposium Series 343; American Chemical Society: Washington, DC, 1987.
(5) Benmakroha, Y.; Zhang, S.; Rolfe, P. *Med. Biol. Eng. Comput.* **1995**, *33*, 811.
(6) Norde, W. *Adv. Colloid Interface Sci.* **1986**, *189*, 267.
(7) Jachimska, B.; Wasilewska, M.; Adamczyk, Z. *Langmuir* **2008**, *24*, 6866.
(8) Tanaka, N.; Nishizawa, H.; Kunugi, S. *Biochim. Biophys. Acta* **1997**, *1338*, 13.
(9) Fritz, M.; Radmacher, M.; Cleveland, J. P.; Allersma, M. W.; Stewart, R. J.; Gieselmann, R.; Janmey, P.; Schmidt, C. F.; Hansma, P. K. *Langmuir* **1995**, *11*, 3529.
(10) Kim, D. T.; Blanch, H. W.; Radke, C. J. *Langmuir* **2002**, *18*, 5841.
(11) RCSB Protein Data Bank, http://www.pdb.mde-berlin.de.
(12) Ohta, R.; Saito, N.; Ishizaki, T.; Takai, O. *Surf. Sci.* **2006**, *600*, 1674.
(13) Lewis, K. B.; Ratner, B. D. *Colloids Surf. B: Biointerfaces* **1996**, *7*, 259.
(14) Tunc, S.; Maitz, M. F.; Steiner, G.; Vazquez, L.; Pham, M. T.; Salzer, R. *Colloids Surf. B: Biointerfaces* **2005**, *42*, 219.
(15) Le, M. T.; Dejardin, P. *Langmuir* **1998**, *14*, 3356.
(16) Casals, E.; Verdaguer, A.; Tonda, R.; Galan, A.; Escolar, G.; Estelrich, J. *Bioconjugate Chem.* **2003**, *14*, 593.
(17) Ta, T. C.; Sykes, M. T.; McDermott, M. T. *Langmuir* **1998**, *14*, 2435.
(18) Verklich, Y. J.; Gorkum, O. V.; Medved, L. V.; Nieuwenhuizen, W.; Weisel, S. W. *J. Biol. Chem.* **1993**, *268*, 13577.
(19) Agnihotri, A.; Siedlecki, C. A. *Langmuir* **2004**, *20*, 8846.
(20) Hall, C. E.; Slayter, H. S. *J. Biophys. Biochem. Cytol.* **1959**, *5*, 11.
(21) Tsapikouni, T. S.; Missirlis, Y. F. *Colloid Surf. B: Biointerfaces* **2007**, *57*, 89.
(22) Lin, Y.; Wang, Wan, L.; Fang, X. *Ultramicroscopy* **2005**, *105*, 129.
(23) Cacciafesta, P.; Humphris, A. D.; Jandt, K. D.; Miles, M. J. *Langmuir* **2000**, *16*, 8167.
(24) Feng, L.; Andrade, J. D. In *Proteins at Interfaces II; Fundamentals and Applications*; Horbett, T. A., Brash, J. L. , Eds.; Maple Press: York, PA, 1995; pp 66−79.

10.1021/la803662a CCC: $40.75
Published on Web 02/19/2009

ods.[25−30] Because attention in most of these works was focused on the topology of molecules at surfaces, the influence of parameters characterizing protein solutions was rarely controlled or systematically investigated. This decreased definitely the precision of the topological measurements and made it difficult to compare results obtained in various laboratories.

Systematic measurements of the fibrinogen deposition were performed by Ortega-Vinuesa et al.,[30,31] who measured the thickness of the protein layer on silicon plates by ellipsometry as a function of the solution pH and ionic strength. The highest coverage of fibrinogen, equal to 11 mg/m^2 was observed for pH close to the isoelectric point (iep) equal to 5.8, whereas for pH 9 it was much lower, equal to 1.8 mg/m^2, and 2 mg/m^2 for pH 4.

Precise kinetic measurements of fibrinogen adsorption on silicon and glass surfaces were performed using the in situ fluorescent TIRF technique of Toscano and Santore.[32] These results were supplemented with an interesting AFM study of the topology of single Fb molecules carried out for the low-coverage regime, which clearly demonstrated a trinodular structure of adsorbed molecules.

However, despite the major significance of such studies, there seem to be no results reported in the literature concerning the shape of the molecule, its effective length, uncompensated charge, and stability in electrolyte solutions under various ionic strengths and pH values. Thus, the main goal of this work was to determine these parameters, which have fundamental significance for predicting the kinetics of fibrinogen deposition and its monolayer density at various surfaces. We apply the dynamic light scattering (PCS) and dynamic viscosity methods, which are particularly sensitive in the case of elongated molecules such as fibrinogen.

Materials

Fibrinogen from bovine plasma, fraction I, type IV (65% protein, containing approximately 25% sodium chloride and approximately 15% sodium citrate), was purchased from Sigma (F4753) and used without further purification. The purity of the Fb solution was checked by the dynamic surface tension measurements carried out using the pendant drop shape method. As can be seen in Figure 1, there was practically no change in the surface tension of the 10 ppm solution of Fb within 40 minutes, which is much longer than the typical time of PCS and viscosity measurements, lasting 5−10 min.

Ruby muscovite mica obtained from Continental Trade was used as substrate and was freshly cleaved immediately prior to use. Water was purified using a Millipore Elix 5 apparatus. Chemical reagents (buffers, electrolytes) were of analytical grade and used without further purification. Protein solutions of fibrinogen concentration in the range of 1−1000 ppm were prepared in the same way: the protein powder was dissolved in appropriate (NaCl, phosphate buffer, carbonate buffer, water) solution, mixed gently on a magnetic stirrer, and then filtered with a Millex-GS 0.22 μm filter to eliminate aggregates and impurities. The temperature of experiments was kept constant at 293 ± 0.1 K.

(25) Sit, P. S.; Marchant, R. E. *Thromb. Haemost.* **1999**, *82*, 1053.
(26) Marchin, K. L.; Berrie, C. L. *Langmuir* **2003**, *19*, 9883.
(27) Wigren, R.; Elwing, H.; Erlandsson, R.; Welin, S.; Lundström, I. *FEBS Lett.* **1991**, *280*, 225.
(28) Green, R. J.; Davies, J.; Davies, M. C.; Roberts, C. J.; Tendler, S. J. B. *Biomaterials* **1997**, *18*, 405.
(29) Sit, P. S.; Marchant, R. E. *Surf. Sci.* **2001**, *491*, 421.
(30) Ortega-Vinuesa, J. L.; Tengvall, P.; Lundström, I. *J. Colloid Interface Sci.* **1998**, *207*, 228.
(31) Ortega-Vinuesa, J. L.; Tengvall, P.; Lundström, I. *Thin Solid Films* **1998**, *324*, 257.
(32) Toscano, A.; Santore, M. M. *Langmuir* **2006**, *22*, 2588.
(33) Adamczyk, Z.; Jachimska, B.; Kolasińska, M. *J. Colloid Interface Sci.* **2004**, *273*, 668.

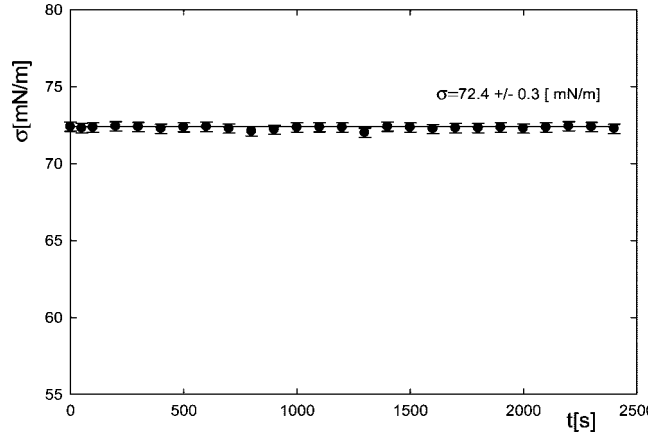

Figure 1. Dependence of the surface tension of fibrinogen solutions σ on time t measured under physiological conditions: pH 7.4, $I = 0.15$ M, and bulk concentration of 10 ppm.

Methods

The diffusion coefficient of fibrinogen under various conditions was determined by dynamic light scattering (DLS), using the Zetasizer Nano ZS Malvern instrument (measurement range of 0.6 nm−3 μm). The Nano ZS instrument incorporates noninvasive backscatter (NIBS) optics. This technique measures the time-dependent fluctuations in the intensity of scattered light, which occur because particles undergo Brownian motion. Analysis of these intensity fluctuations enables the determination of the diffusion coefficients of particles, which are converted into a size distribution. The sample solution was illuminated by a 633 nm laser, and the intensity of light scattered at an angle of 173° was measured by an avalanche photodiode.

Fibrinogen diffusion coefficient (hydrodynamic radius) was determined for one (constant) value of ionic strength equal to 1×10^{-2} M and a pH range from 2.5 to 10. pH was regulated by the addition of HCl or NaOH.

The microelectrophoretic mobility of Fb was measured using the Laser Doppler Velocimetry (LDV) technique (measurement range of 3 nm−10 μm). In this technique, a voltage was applied across a pair electrode placed at both ends of a cell containing the particle dispersion. Charged particles are attracted to the oppositely charged electrode, and their velocity was measured and expressed per unit of field strength as the electrophoretic mobility μ_e. Then, the zeta potential was calculated using Henry's equation

$$\zeta = \frac{3\eta}{2\varepsilon F(\kappa a)}\mu_e \qquad (1)$$

where ζ is the zeta potential of proteins, μ_e is the electrophoretic mobility, ε is the dielectric constant of water, $F(\kappa a)$ is a function of the dimensionless parameter κa, $\kappa^{-1} = (\varepsilon kT/2e^2I)^{1/2}$ is the double-layer thickness, e is the elementary charge, k is the Boltzman constant, T is the absolute temperature, $I = {}^1/_2(\sum_i c_i z_i^2)$ is the ionic strength, c_i the ion concentration, and a is the characteristic dimension of the protein (e.g., its hydrodynamic radius).

The electrophoretic mobility of fibrinogen was determined for ionic strength regulated by the addition of NaCl, which was fixed at 10^{-3}, 10^{-2}, and 0.15 M, respectively, for the pH range of 3−11.

The dynamic viscosity of protein solutions was measured using a capillary viscometer equipped with a conductivity sensor of solution level, according to the procedure described previously in ref 33. The flow rate of the suspension volume $v_{sus} = 10\,\text{cm}^3$, through a capillary with the internal diameter R, was calculated as $\langle V\rangle = v_{sus}/\pi R^2 t$, where t is the time of passing the suspension through the capillary. The averaged shear rate $\langle G\rangle = \langle V\rangle/R$ in the capillary was 1.8×10^2 s^{-1}. The device was calibrated using pure liquids of known viscosity, such as water, butyl and amyl alcohols, or ethylene glycol. The precision of viscosity determination for the range 1−10 mPa·s was estimated to be 0.2%.

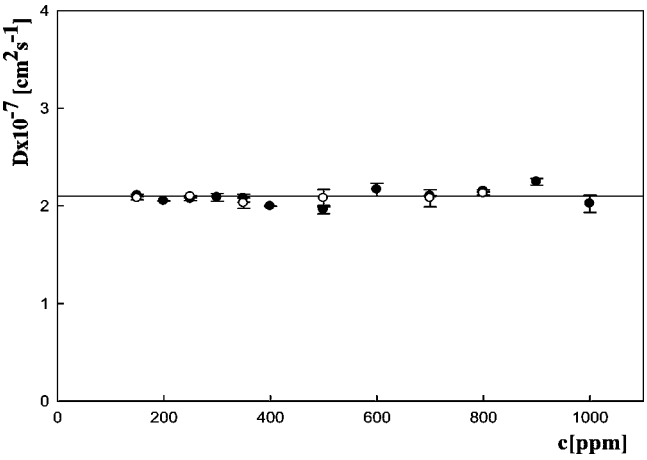

Figure 2. Dependence of the diffusion coefficient of Fb solutions on the bulk concentration c (ppm) determined experimentally for pH 9.5, $T = 298$ K: (●) $I = 5 \times 10^{-2}$ M; (○) $I = 0.15$ M. The line shows the linear fit of experimental points, that is, $D = 2.1 \times 10^{-7}$ cm^2 s^{-1}.

The typical concentration range of Fb solutions in the dynamic viscosity measurements was 100−1000 ppm (solid volume fraction from 7×10^{-5} to 7×10^{-4}), for fixed pH values equal to 3.5, 7.4, and 9.5, and the ionic strength equals 0.15 M. The density of protein solutions needed for a viscosity evaluation was determined by a pycnometer.

PCS measurements were repeated 10−30 times and viscosity measurements, 7 times.

To check that the samples were at steady-state (equilibrium) conditions, all basic physicochemical parameters of fibrinogen solutions such as pH, conductivity, diffusion coefficient, and electrophoretic mobility have been determined as a function of time. Hence, all results presented in this work pertain to the situation in which these parameters were time-independent, within a reasonable time interval of 30−60 min.

AFM measurements have been carried out using the NT-MDT Solver PRO device with scanning head SMENA SFC050L. The measurements were performed in semicontact mode using silicon probe (polysilicon cantilevers with resonance frequencies of 240 kHz ± 10% or 140 kHz ± 10%, typical curvature radius of tip of 10 nm, and cone angle of <20°). The protein solution with Fb concentration equal to 1 ppm was allowed to adsorb on the surface for 5 min, and then substrate was removed, rinsed for 1 h in double-distilled water, and dried under gentle nitrogen stream. The short adsorption time was selected on purpose because in the AFM measurements we were interested in observing individual fibrinogen molecules rather than full monolayer coverage.

Results and Discussion

One of the most important parameters characterizing the dynamics of the protein molecules in solution and their transport kinetics to interfaces is the diffusion coefficient, determined by dynamic light scattering as described above. Knowing the diffusion coefficient, one can calculate the hydrodynamic radius of the protein R_H, which contains important shape information. In Figure 2, the dependence of the diffusion coefficient of Fb on its concentration in the bulk, which was varied within the range from 100 to 1000 ppm is shown. Considering that the specific density of Fb equals 1.38 g cm^{-3} (see Table 1), this corresponds to the range of volume fraction of proteins Φ_V of 3.7×10^{-4}—5.92×10^{-3}. As can be seen, the diffusion coefficient of Fb was practically independent of its bulk concentration, assuming an average value of 2.1×10^{-7} cm^2 s^{-1} for an ionic strength range of 10^{-2}−0.15 M (pH 9.5). This suggests that there were no specific effects stemming from protein aggregation and interactions in the bulk.

Table 1. Physicochemical Properties and Molecular Shape of Fibrinogen

Property \ Protein	Fibrinogen (bovine plasma)
Molecular weight [Da]	340,000
Specific density [g·cm^{-3}]	1.38
Specific volume (v_m) [nm^3]	387
Equivalent sphere radius [nm]	4.5
Postulated molecular dimensions for cylinder [nm]	3.2x3.2x47.5
Diffusion coefficient cm^2 s^{-1}	2.1x10^{-7}
Molecular shape (crystalline state)[11]	

It is interesting that a similar value of the diffusion coefficient of Fb equal to 2×10^{-7} cm^2 s^{-1} was reported by Aptel et al.[34] for the ionic strength of 0.15 M and pH 7.35.

Further measurements of the dependence of Fb diffusion coefficient on pH have also been carried out to determine precisely the range of its suspension stability.

From the diffusion coefficient measurements one can determine the Stokes hydrodynamic radius of the protein using the known dependence

$$R_H = \frac{kT}{6\pi\eta D} \tag{2}$$

where R_H is the hydrodynamic radius, D the diffusion coefficient, and η the viscosity of water.

The advantage of using R_H for interpreting the protein stability is that this quantity is independent of the temperature and viscosity of the suspending medium.

Values of R_H calculated from eq 2 using the measured diffusion coefficients of Fb (bulk concentration = 100 ppm, $I = 0.15$ M) are plotted in Figure 3 as a function of pH. As can be seen, for an alkaline pH range, pH > 8, R_H of Fb attained the limiting value of 12 nm, whereas for the physiological conditions (pH 7.4), the value of R_H was slightly larger, equal to 12.7 nm. As can be seen in Figure 3, there was a Fb instability "window" for 4.5 < pH < 7.5, where the hydrodynamic radius of suspensions increased manifold, attaining values of 100 nm, which indicates unequivocally that a significant aggregation of the protein solutions appeared for this pH range. Similar R_H values (within the experimental error bounds estimated to be 7%) have been observed for lower ionic strengths of 10^{-2} and 10^{-3} M. The results shown in Figure 3 are significant for predicting the optimum conditions for Fb deposition in the form of individual molecules, which are 4.2 < pH > 7.5. Our measurements also explain why so often aggregates are observed in AFM pictures showing Fb monolayers,

(34) Aptel, J. D.; Voegel, J. C.; Schmitt, A. *Colloids Surf.* **1988**, *29*, 359.

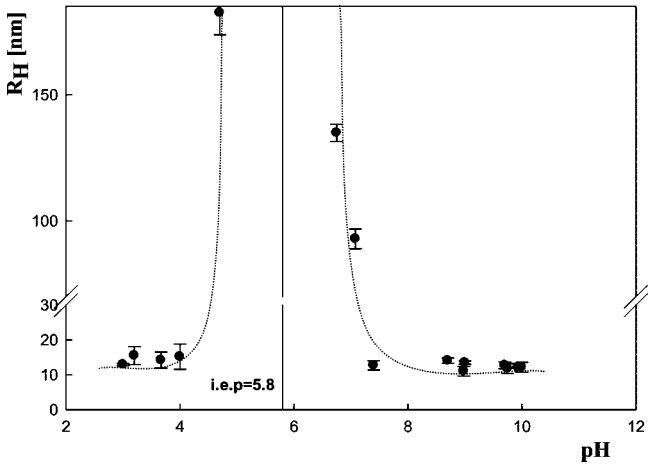

Figure 3. Hydrodynamic diameter R_H of Fb determined by the DLS method as a function of pH, $c = 200$ ppm, $I = 0.15$ M. The dashed line represents nonlinear fit of experimental data.

prepared under uncontrolled condition, such as pure water without buffer, where the pH is likely to fluctuate around 5.5.[23]

Our results shown in Figure 3 are consistent with fibrinogen deposition measurements performed by Ortega-Vinuesa et al.,[31] who determined the thickness of the protein layer on silicon plates by ellipsometry. The highest coverage of fibrinogen reaching 11 mg m^{-2} was measured for pH 5.8, whereas for pH 9 it was 1.8 mg m^{-2} only, and for pH 4, 2 mg m^{-2} g. Because it can be estimated theoretically from random sequential adsorption simulations[35,36] that a monolayer coverage of fibrinogen adsorbing side-on as isolated molecules equals 1.7 mg m^{-2}, these deposition data are consistent with the postulate that for the pH range close to 9 and 4 a monolayer of fibrinogen is formed, whereas for pH close to the isoelectric point mulitlayer deposition was observed.

Because it has not been done before in the literature, we attempt to compare our R_H data of Fb with theoretical predictions stemming from the hydrodynamic model, successfully applied before for polyelectrolytes such as polystyrenesulfonate (PSS), polyallylamine (PAH), and polyacrylic acid (PAA) having very elongated shapes (nominal length to width aspect ratio λ ranging between 40 and 250)[37,38] and for bovine serum albumin (BSA), characterized by the aspect ratio of approximately 2.[7]

The starting point of our analysis is determining the aspect ratio (length to diameter) of fibrinogen, which is a parameter of primary significance for the hydrodynamic theory. This can be done be using the generally accepted value of the Fb length of $L_e = 47.5$ nm[32] and the molecular volume of one molecule v_m equal to 387 nm.[20] From these data one can calculate the averaged diameter of the molecule by assuming a cylindrical shape $d_m = (4v_m/\pi L_e)^{1/2} = 3.2$ nm. Accordingly, the nominal aspect ratio (length to diameter) equals 15, which means that the molecule is very elongated.

It is worth mentioning that in electrolyte solutions the Fb molecules are strongly hydrated as most proteins,[39] which means that its effective diameter becomes slightly larger and consequently the aspect ratio are slightly larger than the above value of d. Assuming that one monolayer of water dipoles

Table 2. Possible Structures of Fibrinogen in Electrolyte Solutions Derived from Hydrodynamic Measurements

STRUCTURE	REMARKS
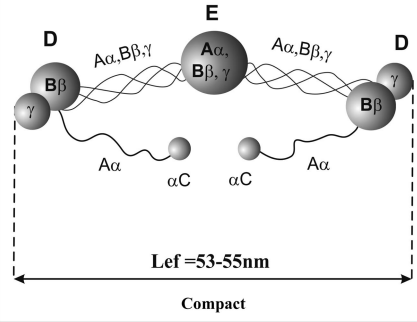	Compact structure appearing for higher ionic strength, e.g. physiological conditions: I = 0.15 M, pH = 7.4, *Nc* = -7.6 *Lc* = 80 nm
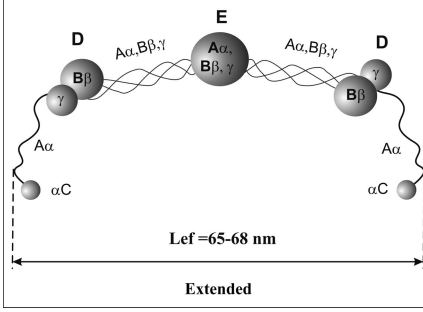	Extended structure appearing for lower ionic strength and pH > 8 *Nc* ~ -26 *Lc* = 80 nm or pH < 4 *Nc* ~ +26 *Lc* = 80 nm

having the length of 0.145 nm[37] is adsorbed uniformly over the Fb molecule, one can expect that the hydrated diameter of Fb $d^* = 3.2$ nm + (2 × 0.145 nm) = 3.5 nm, and the effective aspect ratio λ^* equals 13.6. Knowing the protein dimensions and assuming its cylindrical shape, one can calculate theoretical values of R_H using the hydrodynamic Brenner theory,[41] which predicts the following expression in the limit of aspect ratio $\lambda \gg 1$ (slender body limit)

$$R_H = \frac{L_e}{2(c_1 \ln 2\lambda - c_2)} \tag{3}$$

where $c_1 = 1$ and $c_2 = 0.11$ for cylinders (rods), $c_1 = 11/12$ and $c_2 = 0.31$ for bend cylinders forming a semicircle (semitorus), and $c_1 = 11/12$ and $c_2 = 1.20$ for cylinders bent to the form of a torus (ring).[37]

It can be calculated from eq 3 that in our case $L_e = 47.5$ nm, $\lambda = 13.6$, and $R_H = 7.4$ nm for a straight cylinder and $R_H = 8.7$ nm for a semicircle. As can be noted, these values are noticeably smaller than those experimentally measured, that is, 12 nm for pH 9.5 ($I = 10^{-2}$–10^{-3} M). This comparison suggests quite unequivocally that the contour length of the Fb molecule under these conditions is much larger than this nominal length of 47.5 nm. One can calculate, using eq 3, that the theoretical contour length L_c is 80 nm for a bent cylinder shape (semicircle), which gives $R_H = 12$ nm as the hydrodynamic radius of such a structure. It should be remembered, however, that due to a limiting sensitivity of R_H to L_c, the precision of the above estimate is of the order of 5%.

Hence, from the hydrodynamic radius measurements one can forecast that the most probable configuration of the Fb molecule for pH 9.5 corresponds to that shown in Table 2, which can be approximated by a cylinder of the 80 nm length bent to the form resembling roughly a semicircle.

(35) Schaaf, P.; Talbot, J. *J. Chem. Phys.* **1989**, *91*, 4401.
(36) Talbot, J.; Schaaf, P.; Tarjus, G. *Mol. Phys.* **1991**, *72*, 1397.
(37) Adamczyk, Z.; Bratek, A.; Jachimska, B.; Jasiński, T.; Warszyński, P. *J. Phys. Chem. B* **2006**, *110*, 2426.
(38) Adamczyk, Z.; Jachimska, B.; Jasiński, T.; Warszyński, P.; Wasilewska, M. *Colloids Surf. B* **2009**(in press).
(39) Harding, S. E. *Biophys. Chem.* **1995**, *55*, 69.
(40) Brenner, H. J. *Multiphase Flow* **1974**, *1*, 195.
(41) Norde, W.; Lyklema, J. *J. Colloid Interface Sci.* **1978**, *66*, 266.

As shown before[7,37] the experimental R_H data can be used for determining the uncompensated (effective) charge on molecules as a function of pH and ionic strength, which is the quantity of a primary interest for predicting deposition kinetics and mechanisms on various interfaces.

The effective charge of Fb can be directly derived from the electrophoretic mobility measurements, which give the average translation velocity of the protein V under a given electric field E. Thus, the electrophoretic mobility is defined as $\mu_e = V/E$. As discussed before,[37] knowing the electrophoretic mobility of a particle, one can calculate the averaged number of charges per molecule from the Lorenz−Stokes relationship

$$N_c = \frac{6\pi\eta \times 10^8}{1.602} R_H \mu_e \quad (4)$$

where R_H is expressed in [cm], η in [g·(cm·s)$^{-1}$] μ_e in [μm·cm·s^{-1}·V^{-1}] and V is the volt unit.

It is interesting to mention that eq 4 is more convenient and reliable than the titration methods,[41−43] which tend to largely overestimate the charge on molecules. This is so because of the very likely appearance of ion exchange processes.

Our measurements showed the electrophoretic mobility of Fb under physiological conditions (pH 7.4, $I = 0.15$ M) $\mu_e = -0.51$ μm cm s^{-1} V^{-1}, which gives, using eq 4, the value of uncompensated charge per Fb molecule $N_c = -7.6$. Our estimate is slightly smaller than the literature data of $N_c = -10$.[24] The same effect was observed before in the case of BSA and human serum albumin (HSA),[7] which was attributed to adsorption of counterions, often referred to as ion condensation phenomenon.

For pH values increasing above the physiological level, the electrophoretic mobility of Fb systematically decreased, attaining −1.0 to −1.2 μm cm s^{-1} V^{-1} for pH 9−10 ($I = 0.15$ M), which gives $N_c = -15$ to -18. For lower ionic strength in the range of 10^{-3}−10^{-2} M, the electrophoretic mobility of Fb decreased even more, attaining −1.6 to −2 μm cm s^{-1} V^{-1} for pH 9−10 ($I = 0.15$ M), which gives $N_c = -24$ to -29.

On the other hand, it was determined experimentally that for pH <5.8 the electrophoretic mobility of Fb became positive, meaning that the molecule acquired a net positive charge. For $I = 0.15$, N_c varied between 10 and 17 (for pH 4 and 3) and for $I = 10^{-2}$ M, N_c varied between 21 and 34 (for pH 4 and 3).

As can be seen, the number of charges per Fb molecule attains quite considerable values for pH 3−4 and 8−10 (3 times larger than for BSA and HSA, as determined before using the same method[7]), which practically excludes the possibility of protein aggregation for this pH range, in accordance with the above measurements of the hydrodynamic radius.

It is often more convenient to analyze the electrokinetic behavior of proteins in terms of zeta potential ζ, which is commonly used for the interpretation of colloid, polyelectrolyte, and protein suspension stability.[44] Zeta potential is connected with the measured electrophoretic mobility via constituent dependence, eq 1. In Figure 4 the dependence of the zeta potential of Fb on pH is shown for various ionic strengths. As can be seen, independent of the ionic strength, the zero value of the zeta potential of Fb appeared at pH 5.8, which is usually referred to as the isoelectric point (iep). It is interesting to mention that our value agrees with previous data reported in the literature.[31]

The electrophoretic measurements discussed above suggest that because of a significant charging of the molecule observed for acidic and basic pH at lower ionic strength, one can expect

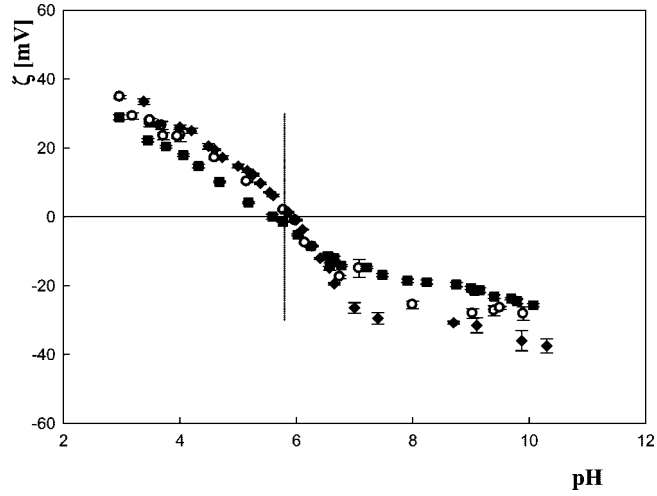

Figure 4. Zeta potential of Fb as a function of pH, $T = 298$ K. The points denote experimental values determined for (◆) natural ionic strength, (○) $I = 1 \times 10^{-3}$ M, and (■) $I = 1 \times 10^{-2}$ M.

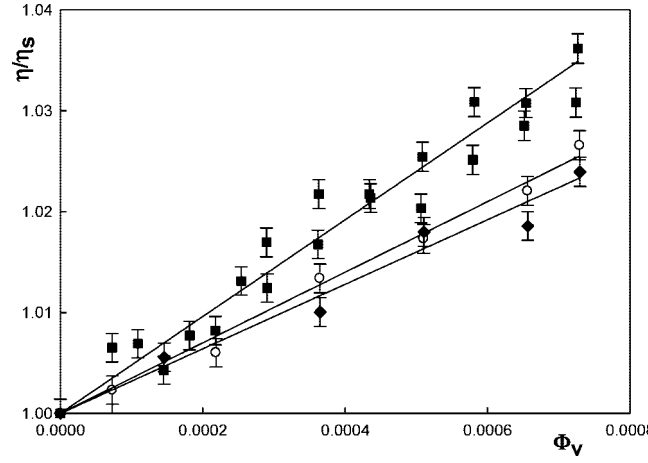

Figure 5. Dependence of the relative viscosity of Fb solutions η/η_s on the volume fraction Φ_V determined for $T = 298$ K, pH 9.5, the points denote experimental data obtained for (■) $I = 10^{-3}$ M, (■) $I = 5 \times 10^{-2}$ M, (◆) $I = 0.15$ M, and (○) pH 7.4, $I = 0.15$ M. The solid lines denote linear fits with the slopes (intrinsic viscosity) equal to 50, 35, and 32, respectively.

significant structural rearrangements of the flexible side arms, analogous to the behavior of polyelectrolyte chains, analyzed in detail in our previous work.[37] Such rearrangements have often been postulated in the literature as interactions of Fb with interfaces during adsorption processes.[22] Information on these structural changes in solutions can be extracted from dynamic viscosity measurements carried out for A low range of volume fractions of protein suspensions.[7]

The slope of the relative viscosity of a suspension η/η_s (where η is the suspension viscosity and η_s is the solvent viscosity) on its volume fraction Φ_V, called the intrinsic viscosity, can be quantitatively related to the shape of molecules or aggregates.

Such dynamic viscosity measurements are shown in Figure 5 for pH 9.5 and various ionic strengths (0.15, 5×10^{-2}, and 10^{-3} M), in the form of the dependence of the relative viscosity of Fb solutions η/η_s on $\Phi_V < 0.008$. As can be seen, the experimental results could be well reflected by the linear dependence with the slope (intrinsic viscosity) equal to 32 for $I = 0.15$ and equal to 50 for $I = 5 \times 10^{-2}$ and 10^{-3} M. By correcting for hydration, assuming a monolayer adsorption of

(42) Galisteo, F.; Norde, W. *Colloids Surf. B: Biointerfaces* **1995**, *4*, 389.
(43) Galisteo, F.; Norde, W. *J. Colloid Interface Sci.* **1995**, *172*, 502.
(44) Adamczyk, Z. *Adv. Colloid Interface Sci.* **2006**, *100−102*, 267.

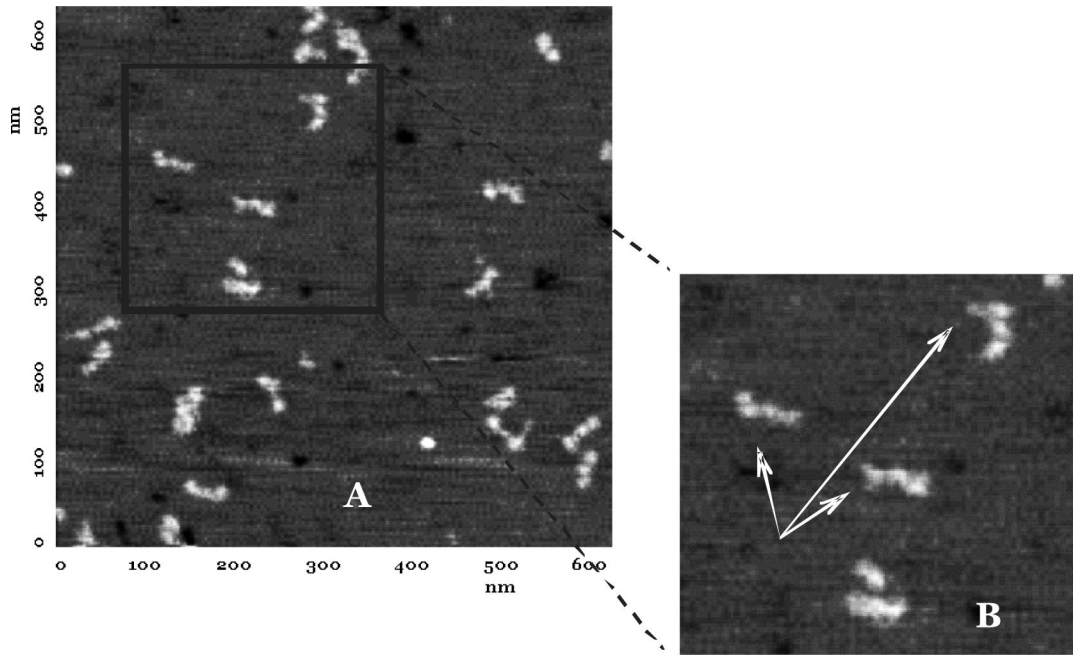

Figure 6. AFM images (tapping mode, air) of single fibrinogen molecules deposited on mica surface (deposition conditions: pH 3.5, $I = 10^{-3}$, $c = 1$ ppm, deposition time = 5 min under diffusion-controlled regime).

water dipoles, having the thickness of 0.145 nm (over the entire protein surface, increasing the apparent volume fraction of Fb), these values become 27 and 42.4, respectively.

On the other hand, fibrinogen suspensions under physiological conditions (pH 7.4, $I = 0.15$) exhibited an intrinsic viscosity of 35, and for pH 3.5, $I = 10^{-2}$ M, the intrinsic viscosity of fibrinogen suspensions was 60. These values should be corrected for hydration as previously done for polyelectrolytes[37] using the formula

$$[\eta]^* = [\eta](\nu_m/\nu_m^*) \tag{5}$$

where υ_m* is the volume of hydrated molecule, equal in our case to approximately $d^{*2}L_e$. In this way one obtains $[\eta]^* = 29.7$ for pH 7.4 and 50.8 for pH 3.5.

It is interesting to compare these results with theoretical predictions stemming from hydrodynamic theories of dilute suspension viscosity. As is well-known, for rigid, spherical particles, the Einstein model predicts that the intrinsic viscosity $[\eta] = 2.5$. This theory has been generalized by Brenner,[40] who considered the case of spheroidal and cylindrical particles immersed in various linear velocity fields. In the case of elongated cylinders, $\lambda \gg 1$ (slender body limit), the intrinsic viscosity can be expressed in terms of the analytical dependence

$$[\eta] = \frac{\lambda^2}{15}\left[\frac{3}{\ln 2\lambda - 0.5} + \frac{1}{\ln 2\lambda - 1.5}\right] + \frac{8}{5} \tag{6}$$

It is interesting to observe that according to eq 6, the intrinsic viscosity of elongated (slender) particle solutions is much more sensitive to the length of the body than the hydrodynamic radius R_H.

From the above determined value of λ^* for a hydrated Fb molecule, one can calculate from eq 6 that $[\eta] = 21.4$, which is significantly smaller than the above experimental values, especially for the low ionic strength. This unequivocally indicates that the effective length of Fb at this pH was significantly larger than the nominal value of 47.5 nm, in accordance with previous suggestions derived from the hydrodynamic radius measurements.

Using the method previously applied in the case of polyelectrolytes,[37] one can calculate the effective length of the molecule from the formula

$$L_{ef} = \left(\frac{4\nu_m\lambda^2}{\pi}\right)^{\frac{1}{3}} \tag{7}$$

where λ was calculated by inversion of eq 6, using the experimental values of the intrinsic viscosity. In this way, it was found that $L_{ef} = 53$ nm for $I = 0.15$ M, which is close to the nominal length of fibrinogen in the crystalline state, equal to 47.5 nm. This estimation suggests that for the higher ionic strength, the fibrinogen molecule assumes a compact structure with the side arms significantly collapsed toward the Fb backbone (see Table 2).

On the other hand, for lower ionic strength, because of a significant charging of the side arms, the Fb molecule assumes a more extended shape having the effective (end to end) length of 64 nm for $I = 5 \times 10^{-2}$–10^{-3} M. On the other hand, a value of 68 nm was found for pH 3.5 and $I = 10^{-3}$ M, which also suggests that the molecule has an extended structure.

These estimations, combined with previous values of the contour length of Fb derived from hydrodynamic radius measurements, allow one to propose the extended structure of fibrinogen such as shown in Table 2. The molecule probably assumes such a structure for the high charge range, that is, for pH > 9 or pH < 4.

The possibility of the existence of Fb in the highly charged, extended state, demonstrated by the hydrodynamic measurements was further supported by the AFM topological observations performed for single molecules adsorbed on bare mica under pH 3.5 and ionic strength of 5×10^{-2} M (see Figure 6). These adsorption conditions have been chosen because, as shown above, fibrinogen molecules were highly positively charged, whereas the mica substrate remained negatively charged, having a zeta potential value of −35 mV.[46] This ensured an irreversible,

electrostatically driven attachment of fibrinogen molecules to the surface, which is very convenient for AFM studies. Moreover, in our AFM studies we were interested in observing isolated fibrinogen molecules, rather than the equilibrium coverage. Therefore, the short 5 min adsorption time was chosen to obtain coverage of ca. 2.5% at a protein concentration of 1 ppm (this value was calculated by assuming the diffusion-controlled transport of protein[44]).

As can be seen, the topology of adsorbed Fb molecules resembles the proposed extended structure, with the effective length attaining 55 nm.

Analogous measurements of this type have previously been done by Cacciafesta et al.[23] for ultraflat oxidized titanium surfaces. The length of the single structures measured on these surfaces varied between 46 and 66 nm.

Similar values of Fb length at mica covered by poly-L-lysine (66 nm)[45] and OTS substrate (64 nm)[25] reported in other works were obtained using the AFM technique.

Conclusions

The hydrodynamic radius of Fb was found to be 12.7 nm for pH 7.4 (physiological conditions) and 12 nm for pH 9.5. These values were consistent with theoretical predictions for slender bodies (cylinders) having the contour length of 80 nm bent to the form of a semicircle.

Using hydrodynamic radius values, the number of uncompensated (electrokinetic) charges on fibrinogen molecules N_c was calculated from the electrophoretic mobility data. It was found that for physiological condition (pH 7.4, $I = 0.15$), $N_c = -7.6$, which is slightly smaller than the previously assumed value of $N_c = -10$. For pH >9 this charge increased (in absolute terms), attaining $N_c = -26$ for $I = 10^{-2}$ M. On the other hand, for pH <4 fibrinogen was highly positively charged, with N_c attaining 26.

It was also determined that the isoelectric point of Fb was 5.8, in accordance with previous experimental data. For the pH range close to the isoelectric point, that is, 4−7, the stability of Fb suspension was found to be low.

These physicochemical characteristics were supplemented by dynamic viscosity measurements, carried out as a function of Fb bulk volume concentration, for various pH values. The intrinsic viscosity data derived from these measurements and the hydrodynamic diameter results were compared with theoretical predictions stemming from Brenner's hydrodynamic model applicable for slender bodies. This allowed one to determine the effective length of the molecule which, under the compact state (high ionic strength), was 53−55 nm and, under the extended state (low ionic strength, pH <4 or >9), 65−68 nm, compared to the nominal length of Fb of 47.5 nm in the crystalline state. This suggested a significant unfolding of the terminal domain chains of Fb caused by the increase in their charge, which was partially confirmed by AFM measurements.

It can be, therefore, concluded that dynamic viscosity and dynamic light scattering measurements can be exploited as a convenient tool for determining the effective length of proteins in electrolyte solutions.

Acknowledgment. This work was financially supported by the COST D43 Special Grant of MNiSZW.

LA803662A

(45) Taatjes, D. J.; Quinn, A. S.; Jenny, R. J.; Hale, P.; Bovill, E. G.; McDonagh, J. *Cell Biol. Int.* **1997**, *21*, (11), 715–726.

(46) Scales, P. J.; Grieser, F.; Healy, T. W. *Langmuir* **1990**, *6*, 582.